JOURNAL OF MATERIALS SCIENCE 27 (1992) 111–121

Fracture mechanism of toughened epoxy resin with bimodal rubber-particle size distribution

T. K. CHEN*, Y. H. JAN
Chemical Engineering Department, National Central University, Chung-Li, 32054 Taiwan

A bimodal rubber-particle distributed epoxy resin was made by simultaneous addition of two kinds of liquid rubbers, CTBN1300X9 and CTBN1300X13. These rubbers were added at a constant total rubber content but with varying weight ratios. The microstructure and fracture behaviour of these rubber-modified epoxy resins have been studied. A strong increase in the fracture resistance was found for the bimodal rubber-particle distributed epoxy resin. The role of the small particle is thought to toughen the shear bands between large particles. The role of large particle is thought to induce a large-scale shear deformation in the crack front. The synergistic effect of these particles gives rise to a strong increase in the toughness of these bimodal rubber-particle distributed epoxy systems.

1. Introduction

Improvement in epoxy toughness had been attributed to a number of fracture mechanisms, including crazing [1–4], rubber tearing [5, 6], shear flow and crazing [7, 8]. Unfortunately, most of the mechanisms have given rise to a great deal of controversy. Most recently, a mechanism which operates through rubber cavitation and matrix shear yielding processes has been proposed [9–11] and well accepted [12–16] in the literature. This mechanism indicates that the greater crack resistance in the rubber-modified epoxy resin arises from two processes. The first is the cavitation at the particle/matrix interface, and the second is the multiple, but localized, plastic shear yielding in the matrix initiated by the stress concentration associated with the rubber particle. Although the energy dissipation processes of the rubber-modified epoxy resin have been illustrated roughly by this mechanism, many microstructural features which might affect these processes have not been very conclusive [11]. A major problem in the elucidation of such a relationship is due to various microstructures which are difficult to vary independently. The effect of bimodal rubber-particle size distribution on the measured fracture toughness is an example in this category. To study this effect, there are two individual works reported in the literature: one adds bisphenol-A to the rubber-modified epoxy system [2, 16, 17]; the other simultaneously adds two kinds of rubber (a solid rubber and a liquid rubber) to an epoxy resin system [9]. The addition of bisphenol-A to a CTBN/piperidine/DGEBA system would induce, during curing, different degrees of chain extension [2] and, finally, the precipitated rubber would result in a bimodal particle size distribution [2, 16, 17] which would centre average particle sizes at 0.1 and 1.3 μm. These systems indeed induce a higher value of fracture energy compared with a conventional rubber-toughened epoxy system with unimodal particle size distribution [2, 16, 17]. However, the enhancement in the case with the bimodal particle size distribution is further complicated by the simultaneous change in the matrix property which arises from the blending of a large amount of bisphenol-A to the resin phase.

Another study on the effect of bimodal particle size distribution was found in the work of Bascom *et al.* [9]. They prepared a rubber-modified epoxy using two kinds of rubber: a reactive liquid rubber (Hycar CTBN1300X13, $\bar{M}_n = 3500$), and a solid rubber (Hycar 1472, $\bar{M}_n = 260\,000$). Their toughened system resulted in a bimodal rubber-particle size distribution, and the fracture energy was higher than that of resins toughened by either kind of rubber alone. However, in Bascom *et al.*'s work, the total content of initially added rubber was not held constant. As their particle size distribution was changed from the unimodal type to the bimodal type, their rubber volume fractions also changed. Because rubber volume fraction is also a major feature in determining the fracture toughness of a rubber-modified epoxy resin, the net effect of the particle size distribution on the toughness might, thus, be complicated.

In this investigation, we attempted to keep the matrix property and total rubber content constant, while varying the relative amounts of large and small rubber particles. Two kinds of reactive liquid rubber with different solubility parameters (CTBN1300X9 and CTBN1300X13) were mixed under fixed total rubber content but at varying weight ratios, into an epoxy resin system. After curing, either kind of CTBN rubber may precipitate individually with their particular particle sizes. Moreover, in accordance with the

*Author to whom all correspondence should be addressed.

0022–2461/92 $03.00+.12

recently accepted "cavitation and shear yielding" fracture mechanism [9–16] and the usage of the newly developed TEM/SEM comparison method for measuring the degree of cavitation [13], the fracture mechanism for toughened epoxy resin with bimodal rubber-particle size distribution will be investigated.

2. Experimental procedure

2.1. Materials

2.1.1. Epoxy resin

The epoxy resin used was Epon 828, which was a liquid diglycidyl ether of bisphenol-A (DGEBA). It was cured by piperidine and used as-received. Casting of epoxy resin was made from 100 p.h.r. resin and 5 p.h.r. hardener. Pre-weighed hardener was slowly added to the resin. The mixture was stirred constantly to ensure thorough mixing. The well-blended mixture was then degassed in a vacuum chamber and, finally, cast between two 6 mm thick glass plates, which were pre-heated at 120 °C. Resin plaques were cured in the glass moulds at 120 °C for 16 h and allowed to cool slowly to room temperature. The experiments described below on microstructural and fracture studies were conducted using specimens machined from moulded resin plaques of unmodified and rubber-modified epoxy resins.

2.1.2. Rubber-modified epoxy resin

Two kinds of reactive liquid rubber were used together to toughen the epoxy resin. One was Hycar CTBN1300X9 (acrylonitrile (AN) = 18%) and the other was Hycar CTBN1300X13 (AN = 26%). Both are liquid random copolymers of butadiene and acrylonitrile with about two carboxyl end groups. The manufacturer's published properties for these rubbers are shown in Table I. Rubber-modified epoxy resins were fabricated with these rubbers in a constant total rubber content of 10 p.h.r. but with varied weight ratios. The weight ratios for CTBN1300X9/CTBN1300X13 were 10/0, 8/2, 5/5, 2/8 and 0/10, respectively. The resin and the rubbers were mixed at 60 °C to improve rubber/resin miscibility. The subsequent stages of fabrication for rubber-modified resin plaques were exactly the same as those described above for the unmodified epoxy resin.

2.2. Microstructural analysis

The microstructure of the cured epoxy materials was investigated using transmission electron microscopy (TEM), differential scanning calorimetry (DSC) and dynamic mechanical analysis (DMA). Specimens for TEM analysis were microtomed from materials which had been machined to a square rod with each edge about 1 mm. Ultra-thin sections of the cured materials were obtained using an ultra-microtome (Reichert-Jung Ultracut-E) and a diamond knife (Micro Star, Standard Type) at an included 50° angle. To avoid the interference of particle curvature while examining the rubber particles, the ultra-thin sections were microtomed to a thickness of less than 100 nm. For the direct examination on the two-phase nature in a rubber-modified epoxy system, the ultra-thin sections were stained for 5 min in a tetrahydrofuran solution containing 1 wt/vol % osmium tetraoxide (OsO_4) as suggested by Riew and Smith [18]. The OsO_4 would react with the unsaturated rubbers to give relatively electron-opaque regions. The microscopy was conducted using a Hitachi H-600-3 TEM. Quantitative analysis on rubber-particle size distribution was based on the Schwartz–Saltykov method [19] which requires transmission electron micrographs containing at least a total of 100 large rubber particles. The volume fraction of the rubbery phase was also calculated from the micrographs using the method suggested by Guy [20].

The DSC analysis was conducted at a heating rate of 20 °C min^{-1} in a DuPont 9900 Calorimeter and was operated over a temperature ranging from − 100 to + 150 °C. The DMA analysis was conducted at a frequency of 110 Hz using a Rheovibron DDV viscoelastometer which operated over a temperature range from − 100 to + 150 °C. The specimens required in DMA analysis were shaped from 3 mm resin plaques by micro-sawing and were polished with fine emery papers of 2000 meshes and 4000 meshes.

2.3. Tensile property measurements

The tensile tests were performed using an Instron 1302 tensometer and an Instron 2620-602 extensometer. The Dumb-bell specimens were cut from 3 mm resin plaques in accordance with the descriptions in ASTM D638-64T. The cross-head speed of the tensometer

TABLE I Properties of Hycar CTBN rubbers

Property	Designation	
	CTBN1300X9	CTBN1300X13
Acrylonitrile content (%)	18	26
Solubility parameter	8.77	9.14
Specific gravity 25/25 °C	0.955	0.960
Carboxyl content, EPHR	0.067	0.057
Functionality	2.4	1.8
Molecular weight, $\bar{M}_n$	3500	3500
Brookfield viscosity (cP) at 27 °C	160000	570000
Glass transition temperature[a], T_g (° C)	− 45	− 30

[a] Glass transition temperatures were taken from the data reported by Manzione and Gillham [22].

was kept constant at 1 mm min^{-1}. The testing temperature was held at 25 °C.

2.4. Fracture energy measurement

In this investigation, the fracture toughness of the experimental materials was measured in terms of the critical strain-energy release rate. G_{Ic}. This value was determined using tapered double cantilever beam (TDCB) specimen which was originally developed by Mostovey *et al.* [21]. These specimens were machined from a 6 mm resin plaques in accordance with the description in Fig. 1. A sharp crack was formed at the base of the slot by carefully tapping a fresh razor blade in the base, thus causing a sharp crack to grow naturally for a short distance ahead of the razor blade. There are two advantages for the TDCB specimen. One is that the recorded loads are independent of crack length. Thereby, the height of every load peak should be the same and each peak can be taken into account for calculating the G_{Ic} values [21]. The other advantage is that the G_{Ic} values can be easily calculated from the following equation

$$G_{Ic} = 4P^2m/Ebb' \quad (1)$$

where P is the load required to propagate the crack, E is the tensile modulus, b is the specimen thickness, b' is the side groove thickness, and m is a constant which depends on shape of the specimen and has a value of 3.27 cm^{-1} in this investigation. The fracture energy test was conducted on an Instron 1302 tensometer with a crosshead speed of 1 mm min^{-1}. The temperature for the test was held at 25 °C.

2.5. Fractography

The fracture surfaces were examined under a Hitachi S-750 scanning electron microscope operated at an accelerating voltage of 20 kV. Prior to examination the fracture surfaces were coated with a thin evaporated layer of gold in order to improve the conductivity of the examined surfaces and prevent electron-charging on them.

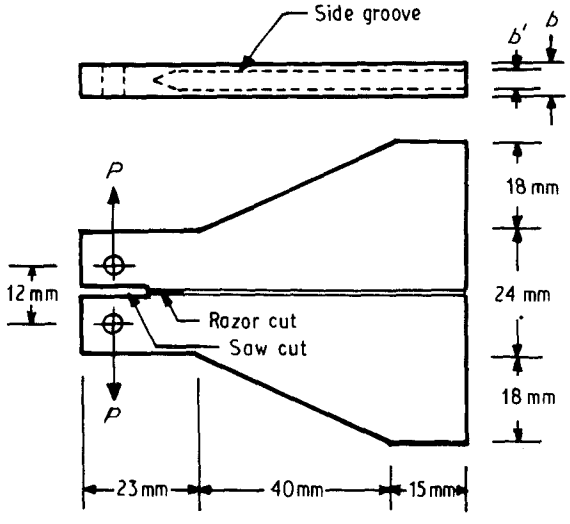

Figure 1 Tapered-double cantilever beam specimen used for fracture energy measurement.

3. Results and discussion

Although the features of the rubbery dispersed phase have a major effect on the toughness of the multiphase rubber-modified epoxy system, there have been few definite conclusions on their effects. In many studies, a crucial feature under investigation may be accompanied by several changes in other features which led to a difficulty in drawing definite conclusions. In this investigation, an attempt was made to establish correlations carefully between the mechanical behaviour and the rubber-particle size distribution.

3.1. TEM studies for morphology of the rubbery phase

3.1.1. Rubber-particle size distribution

Fig. 2a–e are transmission electron micrographs of the epoxy resins toughened with a total of 10 p.h.r. CTBN1300X9 and CTBN1300X13 liquid rubbers at varied weight ratios of 10/0, 8/2, 5/5, 2/8 and 0/10, respectively. From several micrographs containing at least 100 large rubber particles, the particle size distributions for each toughened epoxy system could be calculated using the Schwartz–Saltykov quantitative method [19]. The calculated results are shown in Fig. 3a–e. It was observed that if the resin was toughened by just one kind of rubber, either CTBN1300X9 or CTBN1300X13, the system's particle size distribution would be the unimodal type. Resin toughened with CTBN1300X9 would form large rubber particles with a number average diameter of about 1.9 μm (Fig. 3a) and resin toughened with CTBN1300X13 would form small rubber particles with a number average diameter of about 0.22 μm (Fig. 3e). If the two kinds of rubber were used simultaneously to toughen the epoxy resin, the bimodal rubber particle size distribution would appear in the mixed toughened systems (Fig. 3b–d). The formation of a bimodal rubber-particle size distribution may be deduced for the following reason. While the epoxy resin mixture starts to cure, the molecular weight of the resin will increase, and the CTBN molecule will also react with some epoxy monomer to result in a significant chain extension. Both effects will reduce the total entropy of the mixture and cause precipitation of the rubber. Phase separation begins at the cloud point and ends at the gel point [22]. The ease of phase separation depends on the difference between the solubility parameters of the rubber and the resin. The greater the difference, the easier will be the phase separation. In this investigation, the solubility parameters of CTBN1300X9 and CTBN1300X13 are 8.77 and 9.14, respectively. The difference in solubility parameter between epoxy resin (solubility parameter = 9.70) and the aforementioned rubbers are significantly higher in the CTBN1300X9 system. We might, therefore, conclude that CTBN1300X9 will induce phase separation earlier and will have a longer time allowed for its precipitated rubber particles to coalesce and grow to larger ones before gelation occurs. Because the difference in the rubber-particle size is about an order of magnitude, the large particles formed in the mixed toughened resin will be mostly from CTBN1300X9,

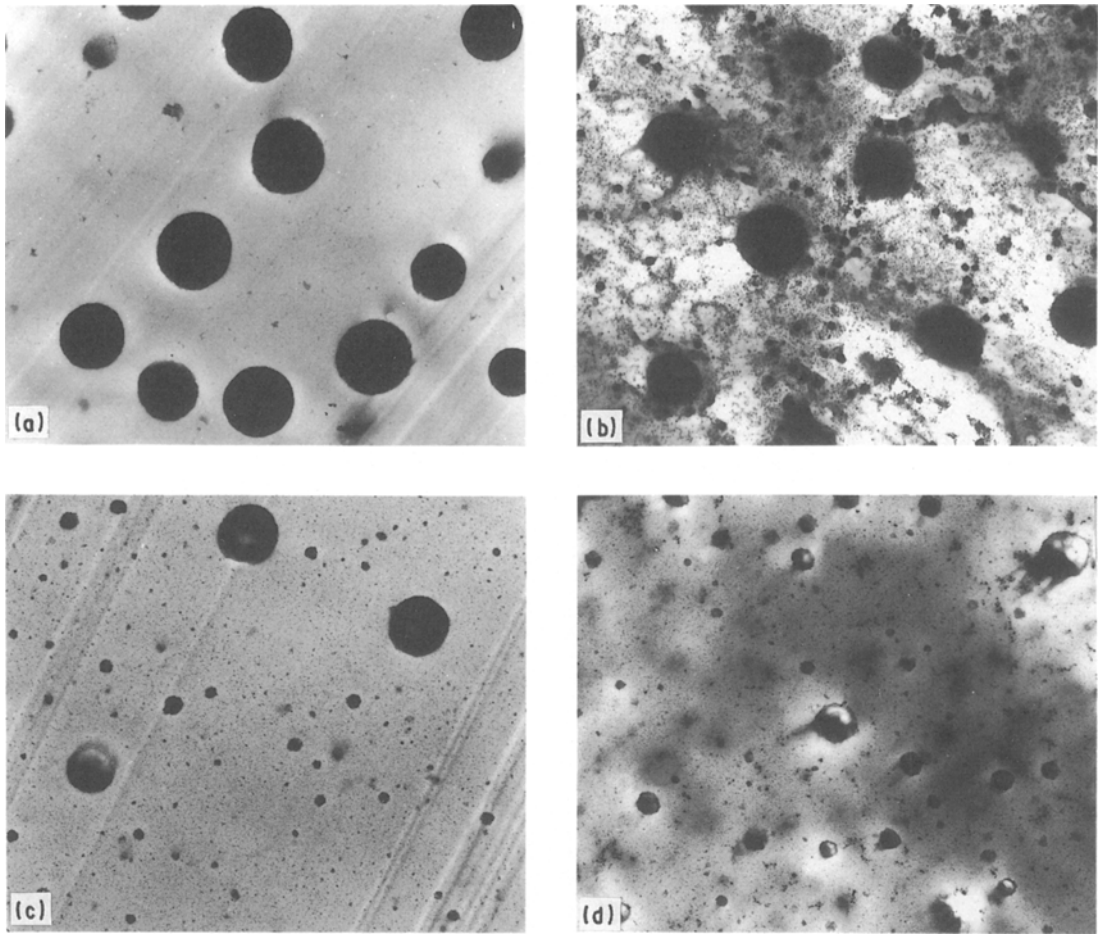

Figure 2 Transmission electron micrographs of microtomed sections from CTBN1300X9 and CTBN1300X13 mixed toughened epoxy resins in which the weight ratios of CTBN1300X9 to CTBN1300X13 (p.h.r./p.h.r.) are: (a) 10/0, (b) 8/2, (c) 5/5, (d) 2/8 and (e) 0/10.

and the smaller particles will be mostly from CTBN1300X13.

3.1.2. Number average particle diameter

The number average particle diameters of the two kinds of rubber particle were individually calculated from each of their particle size distributions in the toughened system. The results are shown in Fig. 4. The average diameter of the large particles increases from 0.98 to 1.90 μm with increasing concentration of CTBN1300X9. The small ones, considered to result from CTBN1300X13, were not affected by varying the concentration of CTBN1300X13, and remained rather constant at the value of 0.20 μm.

These results may be explained by the formation and growth of the rubber particles. The CTBN1300X9 was precipitated early in the cure. Therefore, there is sufficient time for them to grow to large particles by coalescence. Because coalescence will be enhanced by shortening the distance between rubber particles, the larger the concentration of CTBN1300X9, the greater will be the extent of coalescence. This leads to much larger particles for systems with higher concentrations of CTBN1300X9. On the other hand, CTBN1300X13 was precipitated in the later stage of the cure. Owing to the increase in viscosity of the system, there is great difficulty for the particles to coalesce, even though a higher concentration of particles is present.

3.1.3. Rubber-particle number

The number of the small and large rubber particles per unit volume was individually calculated from each of the particle size distributions in each toughened epoxy resin. The results are listed in Table II. It was observed that, the number of large particles was not affected by the amount of CTBN1300X9 and remained constant at the value of about 35 per 1000 μm^3. Nevertheless, the number of small particles increased significantly from 650 to 13 000 per 1000 μm^3 when the content

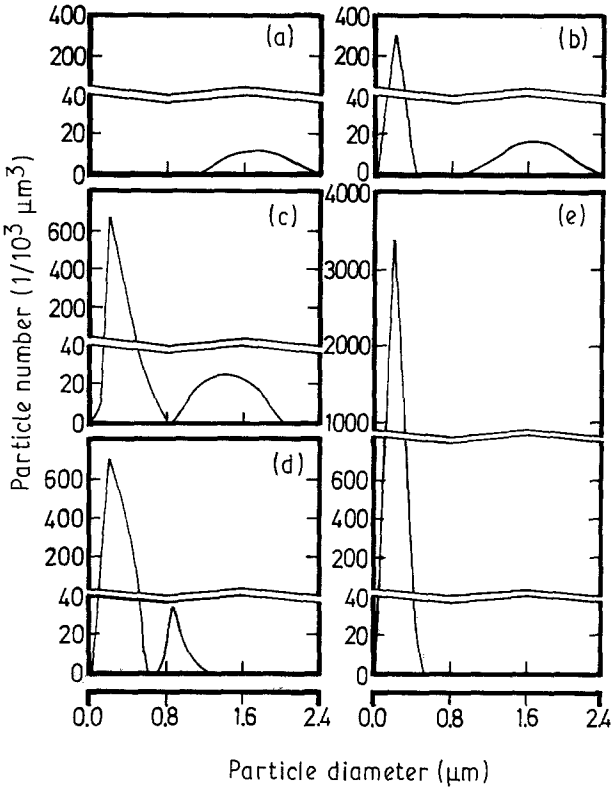

Figure 3 Particle size distribution for CTBN1300X9 and CTBN1300X13 mixed toughened epoxy resins in which the weight ratios of CTBN1300X9 to CTBN1300X13 (p.h.r./p.h.r.) are: (a) 10/0, (b) 8/2, (c) 5/5, (d) 2/8 and (e) 0/10.

TABLE II Number of rubber particles in the CTBN1300X9/CTBN1300X13 mixed toughened epoxy resins

Toughening condition CTBN1300X9/CTBN1300X13 (p.h.r./p.h.r.)	Number of large particles (1/1000 μm³)	Number of small particles (1/1000 μm³)
10/0	32.0	0
8/2	34.5	658
5/5	35.5	887
2/8	40.8	1490
0/10	0.0	13400

of CTBN1300X13 was varied from 2–10 p.h.r. The results are opposite to the tendency shown by the rubber-particle diameter, and might be oppositely explained by the same reasoning.

3.1.4. Volume fraction of the precipitated rubber

The volume fraction of the precipitated rubber is defined as the volume percentage of material enclosed within the boundaries of the rubber particles. The enclosed material includes not only the rubber itself, but also any resin phase which might be trapped inside the particle [7]. It can reveal the degree of phase separation between the rubber domain and the resin matrix [7, 22]. If the volume fraction is less than that of the initially added rubber, some of the added rubber must remain in the resin phase and the phase separation between the rubber and the resin is not complete. The residual rubber will lower the rigidity of the

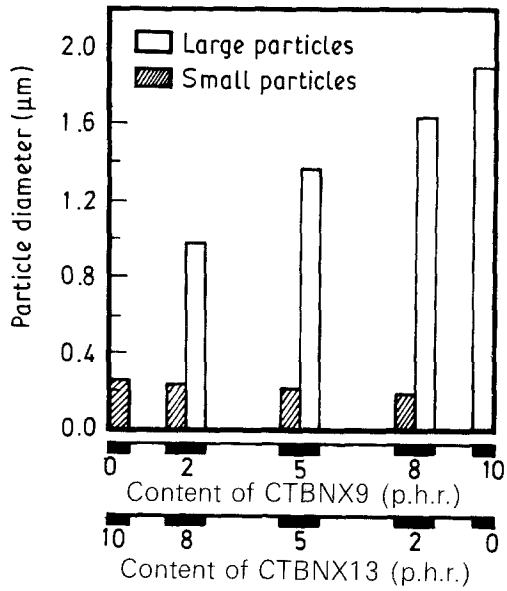

Figure 4 Number average rubber particle diameters in epoxy resin toughened with different weight ratios of CTBN1300X9 to CTBN1300X13.

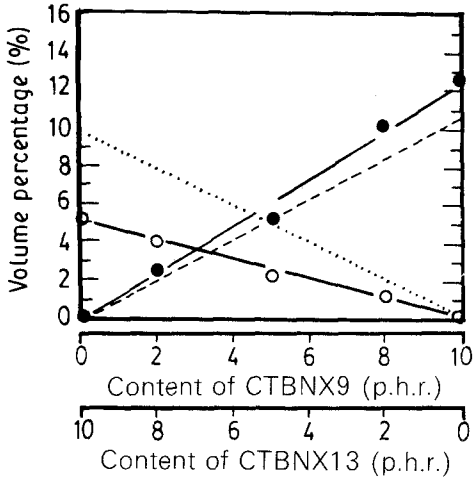

Figure 5 Rubber volume fraction of epoxy resins toughened with different weight ratios of CTBN1300X9 to CTBN1300X13: (●) volume fraction of precipitated CTBN1300X9, (– – –) volume fraction of initially added CTBN1300X9, (○) volume fraction of precipitated CTBN1300X13, (· · ·) volume fraction of initially added CTBN1300X13.

matrix and change its properties. If the volume fraction is higher than that of the initially added rubber, the phase separation is considered to be complete and the matrix properties will not be changed. Even more, in the latter case, there may be some resin subincluded in the rubbery domain. In this investigation, rubber volume fractions of each epoxy system were calculated separately from the transmission electron micrographs by the method suggested by Guy [20]. The results are shown in Fig. 5. It was observed that the volume fraction of the precipitated CTBN1300X9 is always higher than the volume fraction of the initially added CTBN1300X9. On the contrary, the volume fraction of the precipitated CTBN1300X13 rubber is always lower than the volume fraction of initially added CTBN1300X13. The above results indicate that the phase separation between

CTBN1300X9 domain and resin matrix is complete, but for the CTBN1300X13 it is incomplete. The explanation for this follows similar reasons as discussed in Section 3.1.2 for the formation and growth of rubber particles. For the CTBN1300X9 rubber, due to its early precipitation during cure, the phase separation is completed before gelation. On the other hand, the CTBN1300X13 rubber has better compatibility with the epoxy resin, and it may precipitate near the end of B-stage curing. Some of them might remain soluble in the resin matrix as gelation occurs. This part of the rubber might cause some deterioration of the resin's thermal property. Incidentally, as gelation occurs, both the chain-extended rubber and the epoxy resin grow very quickly in size. The fast decrease in the entropy or the fast increase in the molar volume of the mixture might squeeze some rubber molecules out of the resin phase and form many tiny rubber residues. This can be further identified by observing the transmission electron micrographs in Fig. 6b–d for systems containing CTBN1300X13 rubber. It can be observed that there are many rubber nuclei remaining in the resin matrix as shown by the very small electron-opaque spots. This can be further illustrated in Fig. 7, which is a transmission electron micrograph of very high magnification for the epoxy system toughened only by CTBN1300X13. Both the dissolved rubber and the tiny rubber nuclei cannot be accounted for by the volume fraction. The resulting volume fraction for CTBN1300X13 is reduced, accordingly.

3.2. Thermal property of the matrix

The thermal property of the resin matrix was studied by differential scanning calorimetry (DSC) and dynamic mechanical analysis (DMA). The results from DSC and DMA are listed in Table III. The glass transition temperatures of the resin matrix (T_{gm}) from DSC decrease slightly when the content of CTBN1300X13 in each toughened resin is increased, but the decrement is not significant. The matrix T_g from DMA analysis shows the same behaviour as that observed in the DSC analysis. This slight decrement of T_{gm} may indicate a very small amount of rubber still remaining in the resin phase. Because the decrement is not significant, this feature of the matrix phase is taken to be constant during the course of this study. In addition, it was found that there are two low-temperature T_gs in mixed toughened systems. By comparing the T_g of liquid CTBN1300X13 at $-30\,^{\circ}C$ and the T_g of liquid CTBN1300X9 at $-45\,^{\circ}C$ [22], we may

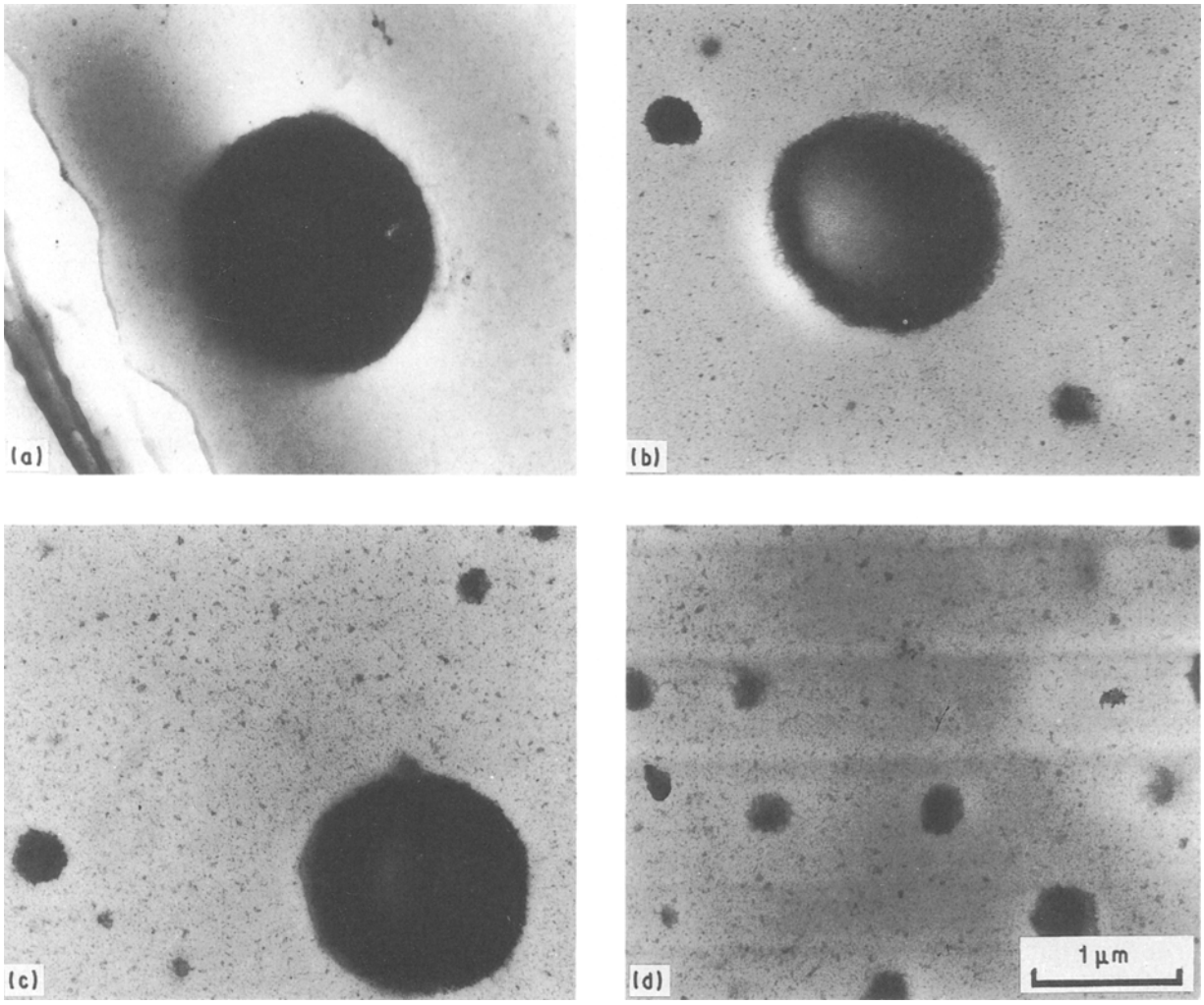

Figure 6 Higher magnification transmission electron micrographs of the microtomed sections from CTBN1300X9 and CTBN1300X13 mixed toughened epoxy resins in which the weight ratios of CTBN1300X9 to CTBN1300X13 (p.h.r./p.h.r.) are: (a) 10/0, (b) 8/2, (c) 5/5 and (d) 0/10.

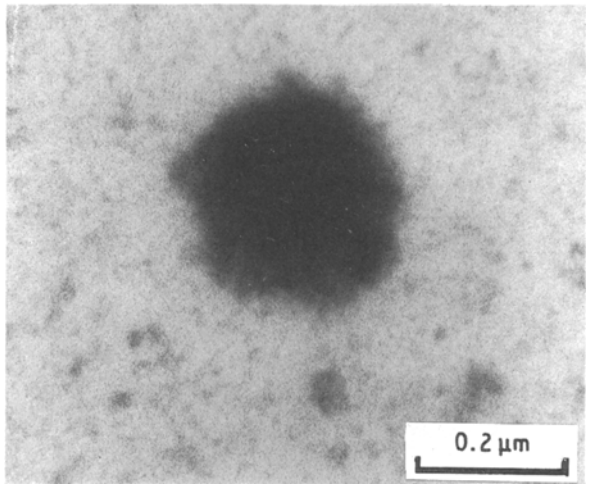

Figure 7 Transmission electron micrograph of a microtomed section of the epoxy resin toughened with 10 p.h.r. CTBN1300X13.

TABLE III Glass transition temperature of CTBN1300X9/CTBN1300X13 mixed toughened epoxy resin

Toughening condition, CTBN1300X9/CTBN1300X13 (p.h.r./p.h.r)	T_{gm}[a] (°C) (DSC)	T_{gm}[a] (°C) (DMA)	T_{gd}[b] (°C) (DMA)
10/0	87	113	− 54
8/2	87	–	–
5/5	85	113	− 49, − 38
2/8	84	–	–
0/10	83	112	− 36

[a] The T_g of the resin matrix.
[b] The T_g of the rubbery domain.

conclude that the higher rubbery phase glass transition temperature at − 38 °C belongs to the T_g of CTBN1300X13 and the lower one at − 49 °C belongs to the T_g of CTBN1300X9. Because these two T_gs are well separated and are close to their original T_gs, this may indicate that these two kinds of rubber precipitated quite individually during the A-stage curing.

3.3. Mechanical properties

3.3.1. Tensile properties

Figs 8 and 9 show the results of yield stress and Young's modulus for the mixed toughened epoxy resins. These properties are quite constant with varying relative quantity of the two liquid rubbers. When the content of CTBN1300X13 increases from 0 to 10 p.h.r., the yield stress is held at about 59 MPa and the Young's modulus shows a slight decrement from 1.97 to 1.83 GPa. Two conclusions may be drawn from the above results. The first, the distribution of the particles does not affect yield stress and Young's modulus. The second, there is some CTBN1300X13 rubber dissolved in the resin matrix as indicated by the slight decrement in Young's modulus, which coincides with the slight decrement in matrix T_g as described above. In observing the stress–strain behaviour for each toughened epoxy resin, there are two other tensile properties worth noting. One is the stress

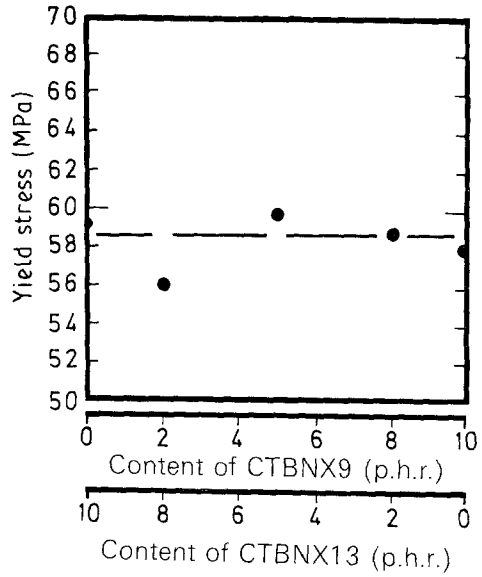

Figure 8 Dependence of yield stress on rubber composition for CTBN1300X9 and CTBN1300X13 mixed toughened epoxy resins.

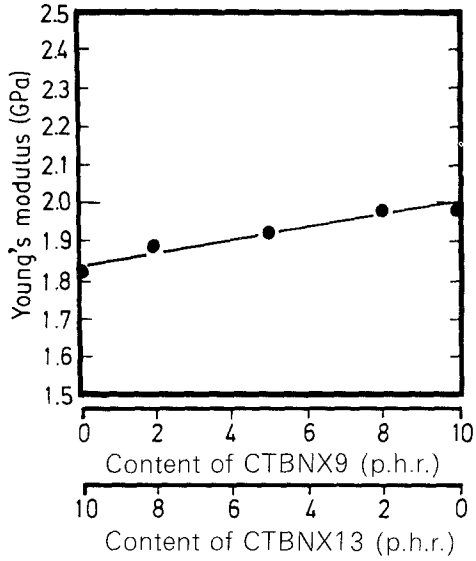

Figure 9 Dependence of Young's modulus on rubber composition for CTBN1300X9 and CTBN1300X13 mixed toughened epoxy resins.

at break and the other is the elongation at break. These two properties are shown in Figs 10 and 11, respectively. It can be observed that resin toughened by two rubbers will exhibit a higher stress at break and higher elongation at break than those toughened by only one kind of rubber. In this work, both the maximum stress at break and the maximum elongation at break appear for epoxy resins toughened with 5 p.h.r. CTBN1300X9 and 5 p.h.r. CTBN1300X13. This indicates that the toughened systems with bimodal rubber-particle size distribution can dissipate more strain energy through higher values of stress and elongation after yielding, i.e. they are more resistant to break through the formation of a localized shear yielding [5]. This is important to understand the influence of bimodal rubber-particle size distribution on the fracture mechanism and will be further discussed later.

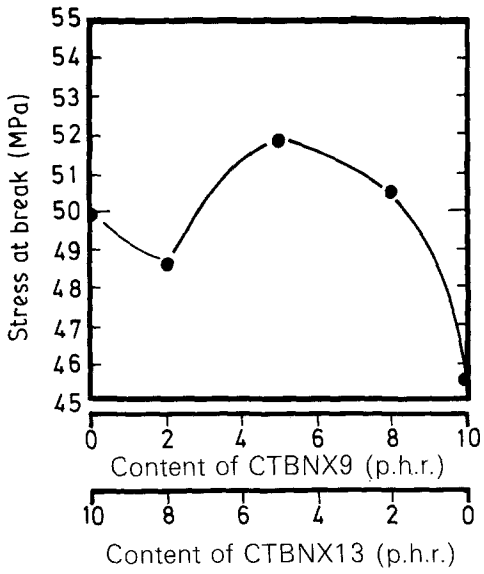

Figure 10 Dependence of stress at break on rubber composition for CTBN1300X9 and CTBN1300X13 mixed toughened epoxy resins.

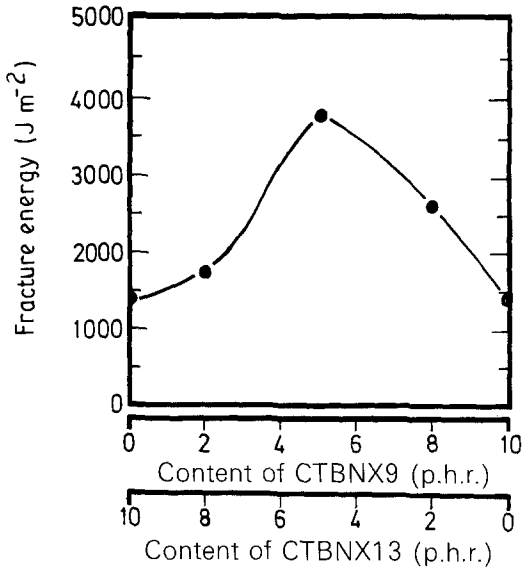

Figure 12 Dependence of fracture energy on rubber composition for CTBN1300X9 and CTBN1300X13 mixed toughened epoxy resins.

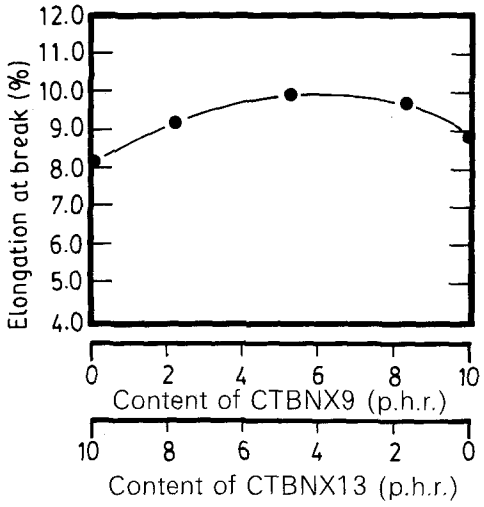

Figure 11 Dependence of elongation at break on rubber composition for CTBN1300X9 and CTBN1300X13 mixed toughened epoxy resins.

3.3.2. Fracture energy

The fracture energy (G_{1c}) was measured from TDCB specimen and calculated from Equation 1. The results for resins toughened with different weight ratios of CTBN1300X9 to CTBN1300X13 are plotted in Fig. 12. A dramatic tendency is observed. Those resins toughened with two kinds of rubber exhibit much higher G_{1c} values than those toughened with only one kind of rubber. The maximum G_{1c} appears in the system with 5 p.h.r. CTBN1300X9 and 5 p.h.r. CTBN1300X13, and reaches the value of 3800 J m^{-2}. This value is about 2.7-fold higher than the systems toughened with only either CTBN1300X9 or CTBN1300X13. The results from fracture energy tests elucidate four important facts. First, resin slightly flexibilized by a small amount of rubber (such as that toughened by 10 p.h.r. CTBN1300X13) does not show a higher value of fracture energy. This indicates that the slight increase in matrix flexibility is not a major feature for the toughness of rubber-modified epoxy resin in this investigation. Second, resin containing the highest rubber volume fraction (such as that with 10 p.h.r. CTBN1300X9) does not show the highest fracture energy. Therefore, the slightly higher rubber volume fraction is not also a major feature in this study of rubber-toughened epoxy. Third, systems with bimodal rubber particle distribution all exhibit much higher G_{1c} values than those with unimodal ones. The bimodal particle size distribution is indeed the prevailing feature compared with other features in the toughness of the rubber-modified epoxy resin. Fourth, a maximum in fracture energy appearing among the mixed rubber toughened systems reveals that there is an optimum bimodal particle size distribution for improving the epoxy toughness. In this investigation, the most advantageous distribution occurs in the system containing 5 p.h.r. of each rubber and in which the average particle diameters for the large and small rubber particles are 1.35 and 0.2 μm, respectively.

3.4. Toughening mechanism for the bimodal rubber-particle distributed epoxy resin

Cavitation at the particle/matrix interface and shear yielding in the matrix are the two most important toughening processes [10–13] which are well accepted and supported by many recent studies [14–16]. Based on this mechanism, the application of a tensile load to a notched specimen would introduce a triaxial stress field ahead of the crack tip. This dilatation causes the cavitation of the rubber particles. Additionally, the rubber particles produce stress concentrations at their equators and also act as sites for the formation of shear bands. The shear bands produced at one particle may terminate at another and keep the yielding localized. Recently, Chen and Jan [23] have experimentally indicated that the cavitation and shear yielding would interact with each other, from their study on the effect of interfacial modification for a rubber-toughened

epoxy resin. From the above discussion, we would first propose that when a tensile load is applied to a notched bimodal rubber particle distributed epoxy resin, a very large stress will concentrate at the equators of large particles, and the small particles which are distributed in between large ones may tend to enhance the shear yielding. The following paragraphs give support for this proposal.

A TEM/SEM comparison technique for measuring the degree of rubber cavitation on the fracture surface was proposed by Yee and Pearson [13] and will be applied in this study. The diameter of the undeformed large rubber particle was obtained from transmission electron micrographs and was discussed in Section 3.1.2. On the other hand, assuming that the rubber particle is broken at the equatorial plane by the crack front, owing to the stress concentration on these planes [11], the rubber-cavity diameter obtained directly from the scanning electron micrographs of the fracture surface of a TDCB specimen can be taken as the cavity diameter resulting from the dilatational deformation of the rubber particle [13]. From comparison of the average diameter of the rubber cavity on the fracture surface and the average diameter of the undeformed rubber particles, the diameter of the rubber cavity is always larger than that of the undeformed rubber particle [10, 12, 13] and the extent of the difference between these two diameters is considered to be the degree of cavitation occurring during fracture [12, 13]. From the data shown in Fig. 13, toughened systems with bimodal particle size distribution exhibit greater cavitation for the large particles. Owing to the interaction between cavitation and shear yielding [23], greater localized shear yielding would also be expected in the matrix where the small rubber particles were distributed. The subsequent questions are: what is the role of a small rubber particle and how does it magnify the degree of cavitation in large rubber particles? To answer these questions, we may start from an examination of crack propagation. When a stress is applied to open up the crack tip, a zone of voids and shear bands is formed ahead of the crack tip.

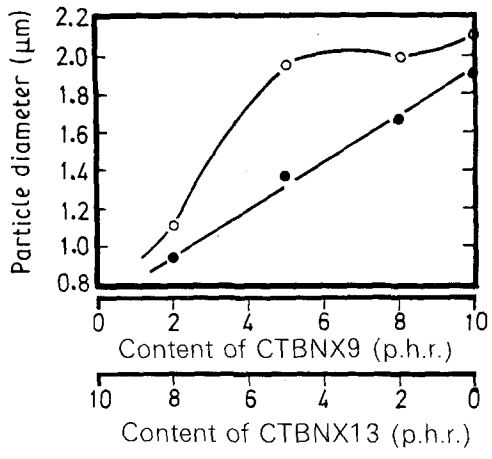

Figure 13 Diameters of the undeformed large rubber particles and diameters of the large rubber cavities as functions of initially added rubber composition: (●) average diameter of the undeformed large rubber particles from TEM, (○) average diameter of the large rubber cavities from SEM.

This voided zone blunts the crack. Further expansion of the crack will result in an even larger voided plastic zone. Eventually, a crack propagates through the voided plastic zone when ligaments between the voids can no longer support the tensile stress. These ligaments are composed of sheared matrix material. A crack, for the most part, will propagate in parallel within the ligament because it's direction has already been imposed by some shear stress. For the bimodal rubber-distributed epoxy resin, small rubber particles distributed in between large ones, they must also distribute within the ligament. It is our hypothesis that the role of the small particle restricts the microcrack to propagate within the ligament, and makes the crack tip region sustain even higher fracture loading by maintaining a higher critical stress level. This higher critical stress level may even generate greater triaxial stress ahead of the crack tip. This produces higher dilatation and causes a higher degree of cavitation in the large rubber particles.

Further evidence for the increase in critical stress level may be found in Figs 10 and 11 where bimodal rubber-particle distributed epoxy resin always show higher values of stress at break and elongation at break. During tensile dilatometry, Yee and Pearson [12] indicated that cavitation will form under the application of tensile expansion and will be followed by the formation of localized shear deformation. Because there is a close relationship between tensile dilatometry and the opening up of a crack tip, we might conclude that the higher values of stress at break, as shown in Fig. 10, would indicate a higher critical stress level as reinforced by the smaller particles included in the shear bands. Because the resulting tensile elongation contributed by the cavitation is probably less than 1%, we might further conclude, therefore, that a higher extent of localized shear deformation, resulting from the higher critical stress level, would cause a higher elongation at break, as shown in Fig. 11.

The above phenomena are believed to be the cause of increasing fracture energy, in the right-hand portion of Fig. 12. When considering the left-hand portion of Fig. 12, we need to consider the effect of particle size in this system. Because the fracture energy of a rubber-modified epoxy resin increases with increasing size of the plastic deformation zone ahead of the crack tip [10, 12], the dependence of the stress whitening length (in the direction of crack propagation) and the stress whitening depth (perpendicular to the direction of crack propagation) on the particle size distribution is worth noting. Fig. 14 shows these results. When the epoxy resin is only toughened by CTBN1300X13, it is toughened by a large number of small rubber particles and the size of the plastic deformation zone (as shown in Fig. 14) is very small (which was examined under SEM analysis). When the epoxy resin is only toughened by CTBN1300X9, it is toughened by a small number of large rubber particles and its plastic deformation zone is quite large. Nevertheless, both of their fracture energies are the same. From these data, we may propose that, for this particular epoxy resin, small particles may produce a highly intense energy

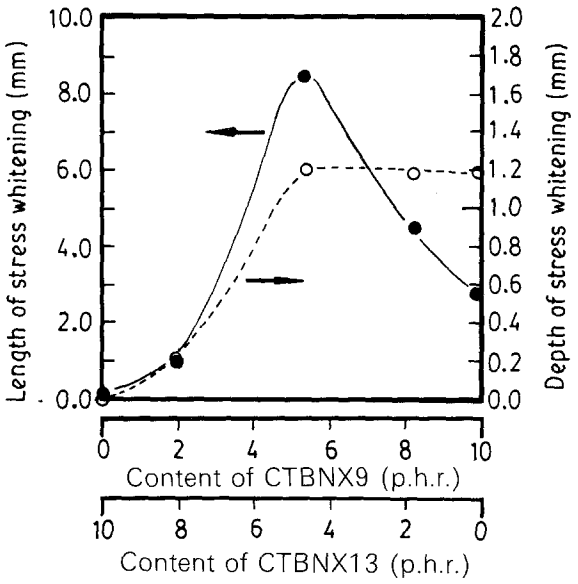

Figure 14 Dependence of length and depth of stress whitening zone on rubber composition for CTBN1300X9 and CTBN1300X13 mixed toughened epoxy resins. (●) Length of the stress whitening zone, (○) depth of the stress whitening zone.

dissipation process, but this process is limited to a small region, and the large particles may produce a less intense energy dissipation process but the process will extend to a large region. From Section 3.1.3, the number of large particles was found to be constant among all the toughened systems, but the particle size increased as the content of CTBN1300X9 increased. Our hypothesis is that, as the size of the large particles increases, the small-scale but highly intense localized shear yielding among small particles may be gradually extended to a large-scale deformation zone, due to the presence of large particles in front of the crack tip. Therefore, in addition to the highly intense plastic deformation occurring among small rubber particles, the role of the large rubber particles was to extend the highly intense deformation to a large size. This causes a greater crack tip blunting and a higher fracture resistance towards the centre of Fig. 12.

Fig. 14 also exhibits a maximum size of the plastic deformation zone for the bimodal rubber-particle distributed epoxy resin. This maximum may indicate that, in addition to the increase in particle size which may enlarge the size of plastic deformation, the increase in the matrix toughenability by the small particles may also play an important role in enlarging the plastic deformation zone.

From the above discussion, it is realized that the role of the small particles and the role of the large particles work by different mechanisms and that an interaction exists. The interaction gives rise to a synergistic toughening effect for the bimodal rubber-particle distributed epoxy system. In this investigation, the optimal interaction was observed at the 5 p.h.r. CTBN1300X13 and 5 p.h.r. CTBN1300X9 toughened epoxy resin system.

4. Conclusions

Two kinds of liquid rubber, CTBN1300X13 and CTBN1300X9, were added simultaneously to an uncured epoxy resin at a total of 10 p.h.r. rubber but with varying weight ratios at 10/0, 8/2, 5/5, 2/8 and 0/10. Microstructural studies indicate that these rubbers precipitate individually to form bimodal-distributed rubber particles during cure. Fracture energy tests reveal a strong increase in the fracture resistance for these bimodal rubber-particle distributed epoxy resins. The optimal increment of fracture energy was found in the system modified by 5 p.h.r. CTBN1300X9 and 5 p.h.r. CTBN1300X13. In this system, CTBN1300X9 forms large rubber particles with an average diameter of about 1.35 μm, and CTBN1300X13 forms small rubber particles with an average diameter of about 0.20 μm. The fracture energy of this rubber-modified epoxy reaches 3800 $J m^{-2}$ and is about 2.7-fold higher than that in a conventional toughened system. The small particle was proposed to toughen the shear band in between the large particles and to give rise to a higher critical stress level for the epoxy resin in between large rubber particles. The higher critical stress level was believed to enhance greater cavitation for the large particles and greater plastic shear yielding on the adjacent matrix before fracture. The large rubber particles were proposed to induce a larger scale of shear deformation when compared with the shear deformation simply caused by the small particles. The synergistic effect of these particles gives rise to the strong increment in the toughness of these bimodal rubber-particle distributed epoxy systems.

Acknowledgement

This research was supported by the National Science Council, Taiwan, under Grant NSC 78-0405-E008-05.

References

1. E. H. ROWE, A. R. SIEBERT and R. S. DRAKE, *Mod. Plastics* **47** (1970) 110.
2. C. K. RIEW, E. H. ROWE and A. R. SIEBERT, *ACS Adv. Chem. Ser.* **154** (1976) 326.
3. J. N. SULTAN, R. C. LAIBLE and F. J. McGARRY, *J. Appl. Polym. Sci.* **6** (1971) 127.
4. J. N. SULTAN and F. J. McGARRY, *Polym. Engng Sci.* **13** (1973) 29.
5. S. KUNZ-DOUGLASS, P. W. R. BEAUMONT and M. F. ASHBY, *J. Mater. Sci.* **15** (1980) 1109.
6. S. C. KUNZ and P. W. R. BEAUMONT, *ibid.* **16** (1981) 3141.
7. C. B. BUCKNALL and Y. YOSHII, *Brit. Polym. J.* **10** (1978) 53.
8. C. B. BUCKNALL, "Toughened Plastics" (Applied Science, London, 1977).
9. W. D. BASCOM, R. Y. TING, R. J. MOULTON, C. K. RIEW and A. R. SIEBERT, *J. Mater. Sci.* **16** (1981) 2657.
10. A. J. KINLOCH, S. J. SHAW, D. A. TOD and D. L. HUNSTON, *Polymer* **24** (1983) 1341.
11. A. J. KINLOGH, in "Structural Adhesives: Developments in Resins and Primer" (Elsevier Applied Science, London, 1986) p. 127.
12. A. F. YEE and R. A. PEARSON, *J. Mater. Sci.* **21** (1986) 2462.
13. *Idem, ibid.* **21** (1986) 2475.
14. A. J. KINLOCH, C. A. FINCH and S. HASHEMI, *Polym. Commun.* **28** (1987) 322.
15. R. A. PEARSON and A. F. YEE, *J. Mater. Sci.* **24** (1989) 2571.

16. A. J. KINLOCH and D. L. HUNSTON, *J. Mater. Sci. Lett.* **6** (1987) 131.
17. G. LEVITA, A. MARCHETTI, A. LAZZERI and V. FROSINI, *Polym. Engng Sci.* **8** (1987) 141.
18. C. K. RIEW and R. W. SMITH, *J. Polym. Sci. A1* **1** (1971) 2739.
19. E. E. UNDERWOOD, "Quantitative Sterology" (Addison-Wesley, Reading, MA, 1970) p. 109.
20. A. G. GUY, "Introduction to Material Science" (McGraw-Hill, New York, 1971).
21. S. MOSTOVOY, P. B. CROSLEY and E. J. RIPLING, *J. Mater.* **2** (1967) 661.
22. L. T. MANZIONE and J. K. GILLHAM, *J. Appl. Polym. Sci.* **26** (1981) 889.
23. T. K. CHEN and Y. H. JAN, *J. Mater. Sci.* to be published.

Received 3 August 1990
and accepted 12 February 1991